Relating Polarimetric Radar Measurements to QLCS Cold Pool Properties and Damage Potential

Anna VanAlstine[1] and Matthew R. Kumjian[1]

aev5019@psu.edu

1. Department of Meteorology & Atmospheric Science, The Pennsylvania State University, University Park, PA

Probing QLCS Properties

Motivation (McDonald and Wiess 2021)

Quasi-linear convective storm systems (QLCSs) are mesoscale convective storm systems that can form year-round and often produce hail, severe winds, and possible tornadoes.

A cold pool is necessary for QLCS progression and plays a role in hazardous production.

- What are the cold pool properties and processes taking place?

- Can processes be attributed to subsequent hazards?

The challenge:

Sampling of the microphysical and thermodynamic properties of QLCSs is challenging and typically unachievable with the current operational observing infrastructure.

Hypothesis

Heterogeneities are suspected to play a role in QLCS hazard production.

Polarimetric radar-based proxies of cold pool properties can illuminate these heterogeneities.

Research Goal: Identify operationally observable proxies that could ultimately lead to a more robust indication of QLCS risk potential.

PERiLS: Propagation, Evolution, and Rotation in Linear Storms

Through the joint efforts of the Propagation and Evolution of Rotation in Linear Systems (PERiLS) project, sampling of the microphysical and thermodynamical properties of QLCSs are achieved.

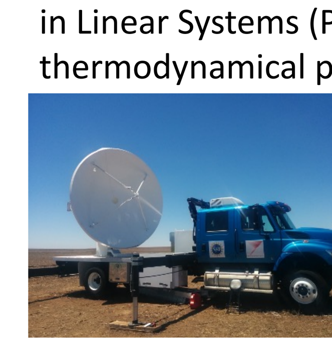

Polarimetric radar data retrieved by Doppler on Wheels (DOW) mobile weather network

Fig 1: (left) DOW mobile Doppler radar truck (FARM)

Thermodynamic data provided by Texas Tech University StickNets

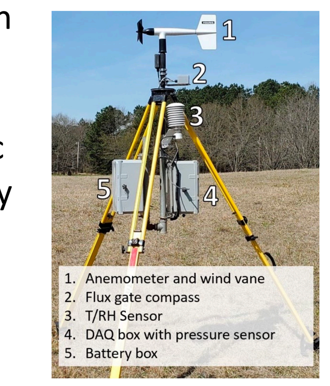

Fig. 2: (left) StickNet with Labeled Components (Texas Tech Univ StickNet Doc. PERiLS 2022)

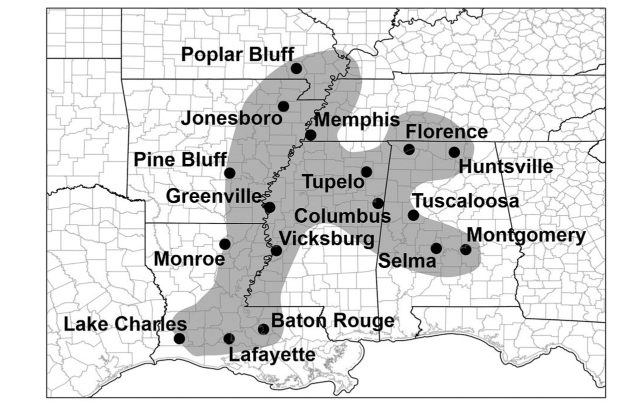

Fig. 3: PERiLS Project Domain (NOAA NSSL)

Quantifying Cold Pool Strength

Spatiotemporal Distribution of Buoyancy Gradients Characterize Variability of Cold Pool Strength.

Using direct StickNet measurements, departures in virtual potential temperature (θ_v') from the environmental "base-state" are calculated to quantify gradients of negative buoyancy

Equation for virtual potential temperature from Bolton(1980)

Multipass objective analysis techniques are employed in interpolation of virtual potential temperature departures to produce contouring of negative buoyancy production.

Multipass objective analysis techniques from Majcen et al. (2008)

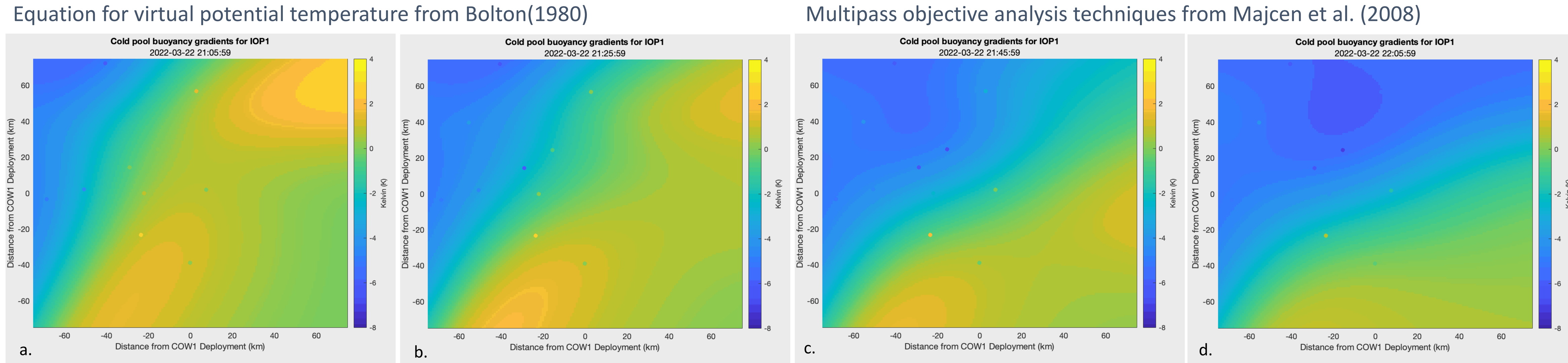

Fig 4 (a-d): Four-panel time series showing variability in cold pool pool strength. Magnitude of cold pool quantified by departures in virtual potential temperature from environmental "base-state". Note the tight gradients along the cold pool's leading edge.

Polarimetric Radar Proxy

We estimate specific attenuation (A) as our polarimetric radar-based proxy of negative buoyancy.

Estimation Ryzhkov et al. (2014)

Specific attenuation estimated from the total usable span of ϕ_{DP} and Z.

$$A = \frac{Z_a^b(r)C(b,PIA)}{I(r_1,r_2)+C(b,PIA)I(r,r_2)}$$

Z_a: Intrinsic reflectivity

b: Constant (usually 0.6-0.9 for microwave frequencies)

$$I(r_1,r_2) = 0.46b\int_{r_1}^{r_2} Z_a^b(s)\,ds$$

(r_1,r_2): Beginning & ending ranges of rain segment in radial (reference range)

$$I(r,r_2) = 0.46b\int_{r}^{r_2} Z_a^b(s)\,ds$$

(r,r_2): Running & reference ranges of radial

$$C(b,PIA) = \exp(0.23bPIA) - 1$$

C: Known 2-way attenuation along propagation path when subject to rain

$$PIA(r_1,r_2) = \alpha[\phi_{DP}(r_2) - \phi_{DP}(r_1)]$$

PIA: Path-integrated attenuation

ϕ_{DP} Span proportional to total path-integrated attenuation

Raindrop drop size distributions (DSDs) and scattering calculations used to estimate α

Specific Attenuation: as radar pulse penetrates an area of precipitation, some of the signals are absorbed and/or scattered

scattering and/or absorption ***per unit distance*** along the propagation path through precipitation

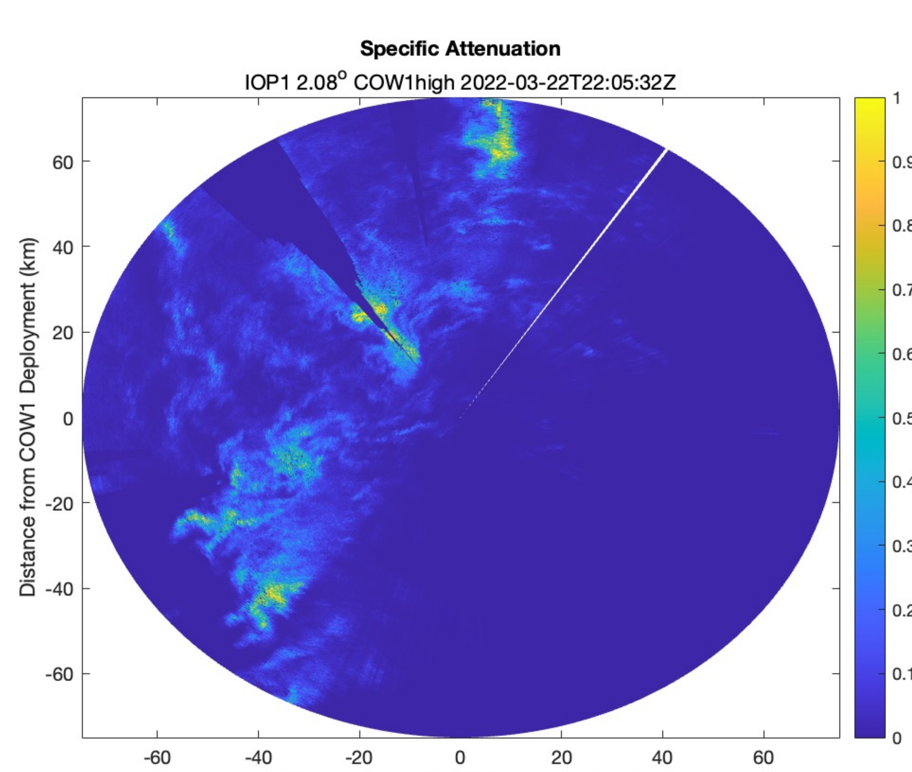

Fig. 5: Field estimates of specific attenuation (A) using C-band DOW data retrieved during the first intensive observational period (IOP 1) of PERiLS 2022 campaign.

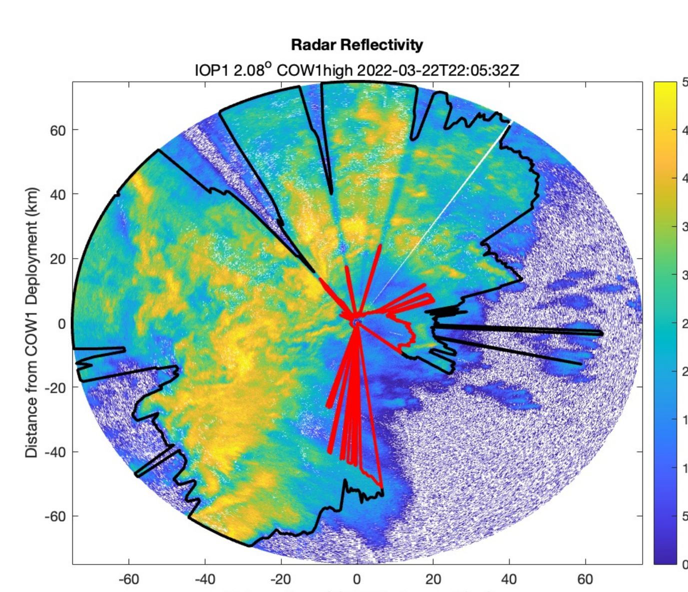

Fig 6: Radar reflectivity field corresponding to estimated A (Fig. 2) from the COW during 2022 IOP1. Beginning and end ranges used in PIA calculation and A estimation for each radial given by the red and black lines, respectively.

Key Takeaways

Greatest enhancement in specific attenuation collocated with largest virtual potential temperature deficit
(specific attenuation enhancements occur along tight virtual potential temperature gradients)

Distribution of buoyancy gradients along leading edge of cold pool imply enhanced baroclinic vorticity
(baroclinic generated vorticity attributed to formation of mesovortices and increased tornado potential)

More robust indication of QLCS risk potential may be achievable by use of specific attenuation as a proxy for QLCS heterogeneities
(which may influence QLCS evolution and possible hazard production)

QLCS Heterogeneities

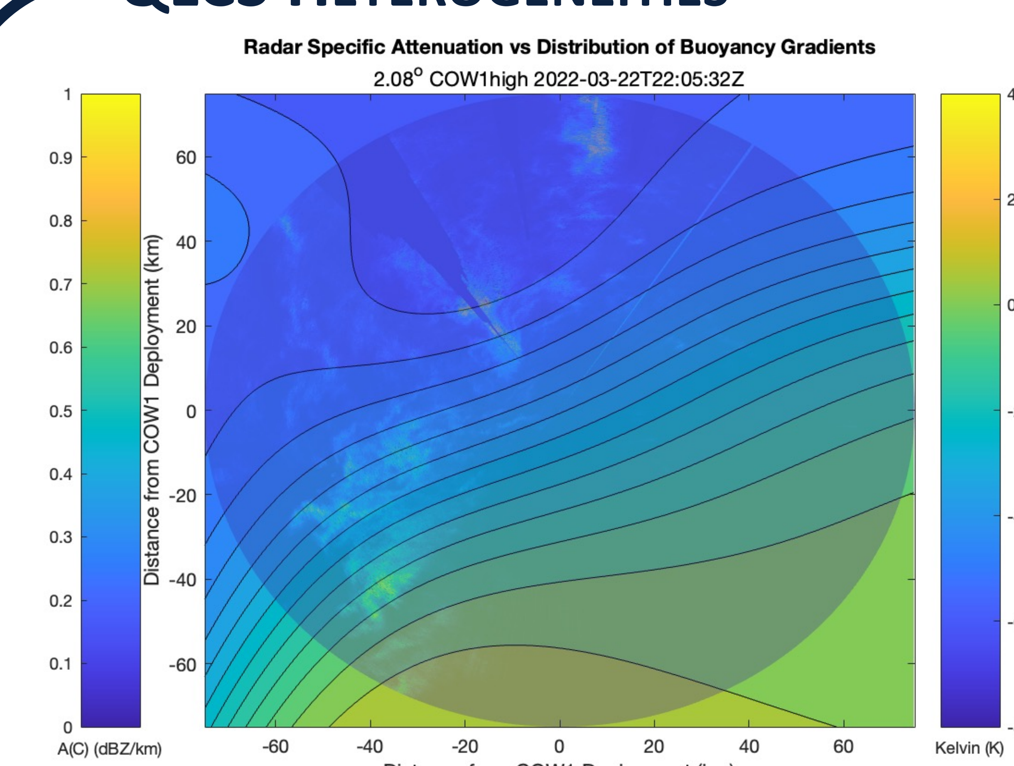

Fig. 7: Estimated of specific attenuation (A, dB/km) overlayed with contours of virtual potential temperature departures (θ'_v , K).

Higher values (warm colors) indicate enhanced attenuation, as well as weaker virtual potential temperature deficits.

Low values (cooler colors) indicate suppressed specific attenuation, as well as stronger virtual potential temperature deficits.

Future Work

Analyze remaining IOP data from 2022 and 2023 field campaigns

Test spatial resolution variability
Estimate specific attenuation field using X-band DOW data
Incorporate more mobile and fixed observational datasets

Apply the idea of "separation vector" between regions of enhanced specific attenuation and enhanced differential reflectivity (Z_{DR})
Separation vectors have been shown to provide information on storm tornadic potential and will be compared to damage reports.

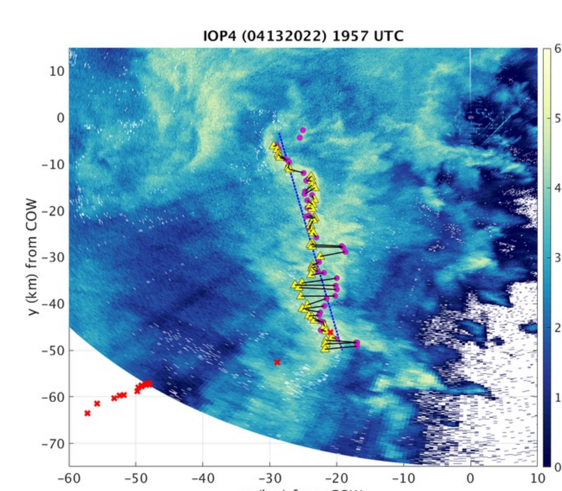

Fig 8: Radar reflectivity field from COW during 2022 IOP4. Separation vectors (black lines) shown between A centroids (yellow triangle) and Z_{DR} centroids (magenta circle) for comparison to locations (red x markers) of damage reports.

References

Bolton, D., 1980: The Computation of Equivalent Potential Temperature. *Mon. Wea. Rev.*, **108**, 1046–1053.

Loeffler, Scott D. and Matthew R. Kumjian. 2018. "Quantifying the Separation of Enhanced ZDR and KDP Regions in Nonsupercell Tornadic Storms." Weather and Forecasting 33 (5): 1143-1157.

Majcen, Mario, Paul Markowski, Yvette Richardson, David Dowell, and Joshua Wurman. 2008. "Multipass Objective Analyses of Doppler Radar Data." *Journal of Atmospheric and Oceanic Technology* 25 (10): 1845-1848,1850,1857-1858.

McDonald, Jessica M. and Christopher C. Weiss. 2021. "Cold Pool Characteristics of Tornadic Quasi-Linear Convective Systems and Other Convective Modes Observed during VORTEX-SE." Monthly Weather Review 149 (3): 821-840.

Ryzhkov, Alexander, Malte Diederich, Pengfei Zhang, and Clemens Simmer. 2014. "Potential Utilization of Specific Attenuation for Rainfall Estimation, Mitigation of Partial Beam Blockage, and Radar Networking." *Journal of Atmospheric and Oceanic Technology* 31 (3): 599-619.

Testud, Jacques, Erwan Le Bouar, Estelle Obligis, and Mustapha Ali-Mehenni. 2000. "The Rain Profiling Algorithm Applied to Polarimetric Weather Radar." *Journal of Atmospheric and Oceanic Technology* 17 (3): 332-356.

Check out the animations!

Funding is provided by the National Oceanic and Atmospheric Administration (NOAA) NOAA 21B053-02